Applied Physics Letters

This article may be downloaded for personal use only. Any other use requires prior permission of the author and AIP Publishing. This article appeared in Tianshun Zhang, Yin Xiao, Wen Chen; Single-pixel microscopic imaging through complex scattering media. Appl. Phys. Lett. 20 January 2025; 126 (3): 031106 and may be found at https://doi.org/10.1063/5.0246489.

RESEARCH ARTICLE | JANUARY 22 2025

Single-pixel microscopic imaging through complex scattering media

Tianshun Zhang ; Yin Xiao ; Wen Chen

Check for updates

Appl. Phys. Lett. 126, 031106 (2025)
https://doi.org/10.1063/5.0246489

View Online
Export Citation

Articles You May Be Interested In

Ghost imaging through complex scattering media with random light disturbance

Appl. Phys. Lett. (January 2025)

Single-pixel imaging through random media with automated adaptive corrections

Appl. Phys. Lett. (April 2025)

Three-dimensional object reconstruction based on spin–orbit interaction of light

Appl. Phys. Lett. (September 2024)

28 May 2025 01:55:27

AIP Publishing

Applied Physics Letters

Special Topics Open for Submissions

Learn More

AIP Publishing

Applied Physics Letters ARTICLE pubs.aip.org/aip/apl

Single-pixel microscopic imaging through complex scattering media

Cite as: Appl. Phys. Lett. **126**, 031106 (2025); doi: 10.1063/5.0246489
Submitted: 1 November 2024 · Accepted: 26 December 2024 ·
Published Online: 22 January 2025

View Online Export Citation CrossMark

Tianshun Zhang,[1] Yin Xiao,[1] and Wen Chen[1,2,a)]

AFFILIATIONS

[1]Department of Electrical and Electronic Engineering, The Hong Kong Polytechnic University, Hong Kong, China
[2]Photonics Research Institute, The Hong Kong Polytechnic University, Hong Kong, China

[a)]Author to whom correspondence should be addressed: owen.chen@polyu.edu.hk

ABSTRACT

Microscopic imaging through complex scattering media is recognized to be challenging. Here, we report high-resolution single-pixel microscopic imaging through complex scattering media. This is developed via an integration of temporal corrections with single-pixel microscopic imaging to enhance the quality of the reconstructed object images and achieve high resolution in complex scattering environments. By adopting a fixed pattern as a temporal carrier, the effect of dynamic scaling factors induced by complex scattering media, which disturb the recorded light intensities, is removed. Artificial targets and biological specimens are tested in optical experiments, and feasibility of the proposed approach is validated to show that the developed single-pixel microscopic imaging system exhibits high robustness against complex scattering. This work offers a promising solution for high-resolution microscopic imaging through thick, dynamic, and complex scattering media.

Published under an exclusive license by AIP Publishing. https://doi.org/10.1063/5.0246489

28 May 2025 01:55:27

Microscopy is pivotal in applied physics, serving as an important tool in many applications, e.g., biological and medical. However, microscopy could face a substantial challenge due to scattering, e.g., biological tissues,[1] which could be thick and dynamic with varying refractive indices.[2] The strong attenuation and complex scattering could lead to a failure of microscopy. Innovative strategies are desirable to overcome the challenge, e.g., single-pixel detection and correlation.[3–6] In recent years, single-pixel imaging,[7] which originated from ghost imaging with entangled light source, has attracted much attention and can reconstruct object images by optically encoding an object using a series of illumination patterns in scattering environments and decoding it via a computational way. This technique inherently possesses anti-interference potential and high sensitivity by recording one-dimensional (1D) total light intensities instead of two-dimensional (2D) patterns with a pixelated camera. The illumination patterns include Fourier basis,[8,9] Hadamard basis,[10] Hermite–Gaussian basis,[11] and mutually orthogonal random matrices.[12] Using a series of orthogonal patterns, single-pixel imaging can achieve satisfactory quality. Single-pixel imaging offers reduced cost, broader wavelength applicability, enhanced sensitivity, and anti-interference capability over optical imaging with pixelated cameras.

When integrated with single-pixel detection, optical microscopy inherits the advantages mentioned above, showing potential in a wide range of applications. An integration of single-pixel detection with microscopy was conducted by Wu *et al.*[13] Over the past years, single-pixel microscopy has been developed with optical information utilization,[14,15] enhanced resolution,[16,17] high adaptability,[18–20] multispectral capabilities,[21–23] multimodality,[24,25] multidimensionality,[26] etc. However, the studies have been mainly conducted on single-pixel optical microscopy without scattering media or with a limited exploration through thin and static scattering media.[27] Therefore, it is crucial and desirable to explore single-pixel optical microscopic imaging through complex scattering media that cause significant spatiotemporal fluctuations in the realizations.

Here, we report an approach to investigating single-pixel microscopic imaging through complex scattering media for achieving high resolution. A complex scattering environment, i.e., thick and dynamic media with varying turbidities, is established in the optical path. It is demonstrated in optical experiments that the resolving power of conventional single-pixel optical microscopy would deteriorate under such complex scattering conditions, and its application is limited. To overcome this challenge, a temporal correction method is designed and applied via an introduced temporal carrier to correct the fluctuations on a series of measured light intensities. The proposed approach enhances the quality of the reconstructed object images in complex scenarios, enabling high-resolution single-pixel microscopic imaging. It is expected that this study would introduce a promising tool for

Published under an exclusive license by AIP Publishing

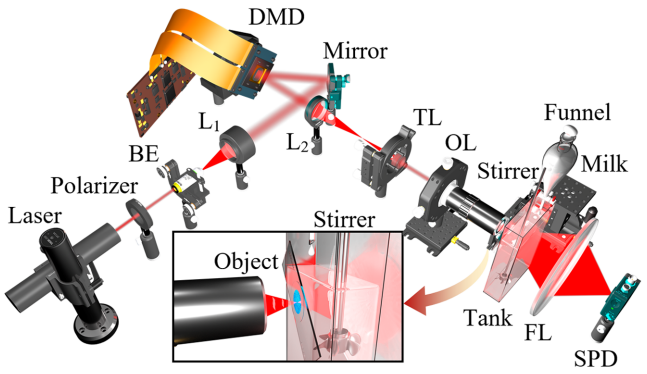

FIG. 1. A schematic experimental setup for the developed single-pixel microscopic imaging through complex scattering media. BE: beam expander; L_1: collimating lens; L_2: lens; TL: tube lens; OL: objective lens; FL: Fresnel lens; and SPD: single-pixel silicon photodiode.

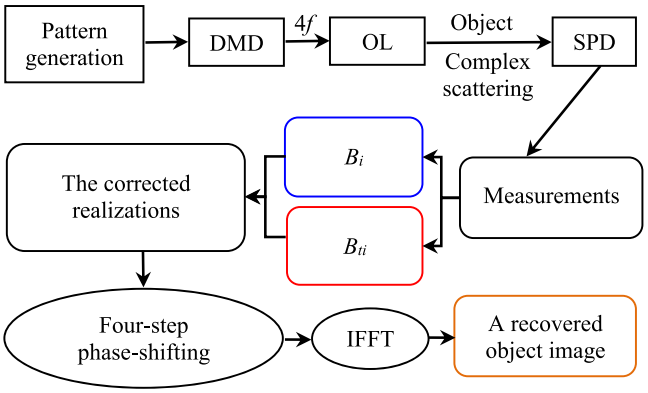

FIG. 2. A flow chart of the proposed single-pixel optical microscopic imaging through dynamic and complex scattering media. OL: objective lens.

high-resolution optical microscopic imaging through complex scattering media in various applications.

A schematic optical setup for the developed single-pixel microscopic imaging through complex scattering media is shown in Fig. 1. A He-Ne laser (wavelength of 632.8 nm and power of 17.0 mW, Pacific Lasertec) emits a linearly polarized beam. The expanded and collimated beam illuminates a digital micro-mirror device (DMD with a pixel size of 10.8 μm, Texas Instruments) at an angle of 24.0° guided by a mirror. The reflected waves propagate through a 4*f* system (a lens L_2 and a tube lens with the same focal length of 20.0 cm) to realize the adjustment of illumination pattern size and then propagate through an objective lens (NA of 0.55 and 50× Mitutoyo). The illumination patterns displayed by DMD are projected onto a target, as shown in the inset. After passing through complex scattering media established by using a water tank (polymethyl methacrylate) with a dimension of 5.0 cm (length) × 10.0 cm (width) × 30.0 cm (height), the optical waves are focused onto a single-pixel silicon photodiode (SPD, PDA100A2 Thorlabs) by a Fresnel lens with 30.0-cm diameter and 12.0-cm focal length. The water tank is placed close to the test target and is filled with 1000.0-ml clean water. To prepare the milk emulsion, 20.0-ml skimmed milk is mixed with 200.0-ml clean water, and then, diluted milk is used via a funnel. During optical experiments, the diluted milk is continuously dripped into water tank. In addition, a motor-driven stirrer agitates the liquid inside water tank at a speed of 450.0 revolutions per minute, emulating a dynamic and turbulent environment with a thickness of 5.0 cm and varied turbidities.

A temporal correction is designed and applied in the developed single-pixel optical microscopy, as shown in Fig. 2. When optical

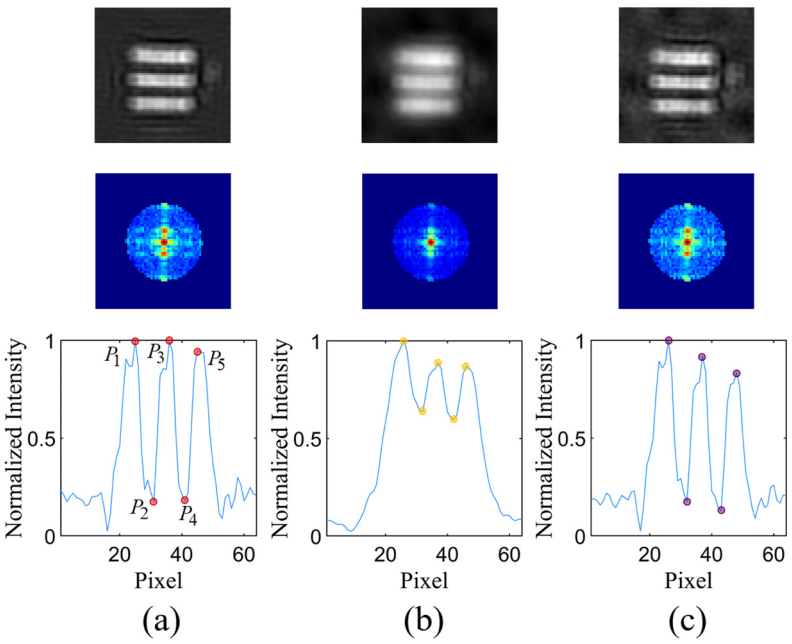

FIG. 3. Experimental results (Group 5 Element 5 of USAF 1951 resolution test chart): A reconstructed object image (64 × 64 pixels), the selected spectra (25% used here), and a normalized intensity curve along the 32nd column of the reconstructed object image when the microscopic imaging is conducted through (a) static and clean water in the optical path, (b) complex scattering media without temporal carriers, and (c) complex scattering media with temporal carriers.

28 May 2025 01:55:27

Published under an exclusive license by AIP Publishing

waves propagate in free space without scattering media, a realization $\hat{B}_i$ $(i = 1,2,3,\ldots)$ collected by the SPD, i.e., single-pixel light intensity, can be described by

$$\hat{B}_i = \int\int I_i(x,y)G(x,y)dxdy, \tag{1}$$

where $I_i(x,y)$ denotes an illumination pattern for the ith measurement and $G(x,y)$ denotes a target. If the same illumination pattern is repeatedly employed, the collected light intensity can be considered as a constant ρ described by

$$\int\int T(x,y)G(x,y)dxdy = \rho, \tag{2}$$

where $T(x,y)$ denotes one fixed pattern.

In the developed single-pixel optical microscopic imaging through complex scattering media, the fixed pattern $T(x,y)$ is pre-generated and alternately displayed by DMD just after each dithered sinusoidal pattern, acting as a temporal carrier. Owing to complex scattering media, a series of dynamic scaling factors k_i are introduced to disturb the light intensities, and the realizations B_i can be described by

$$B_i = k_i \int\int I_i(x,y)G(x,y)dxdy, \tag{3}$$

where a series of sinusoid patterns [see Eq. (S1) in the supplementary material] are sequentially displayed by DMD.

As the fixed temporal carrier $T(x,y)$ is alternately applied, the realizations B_{ti} can be correspondingly described by

$$B_{ti} = k_{ti} \int\int T(x,y)G(x,y)dxdy, \tag{4}$$

where k_{ti} denotes a scaling factor when the temporal carrier is used. Since DMD is employed in the optical setup, it can be reasonably assumed to have $k_i \approx k_{ti}$. Therefore, the realizations B_i

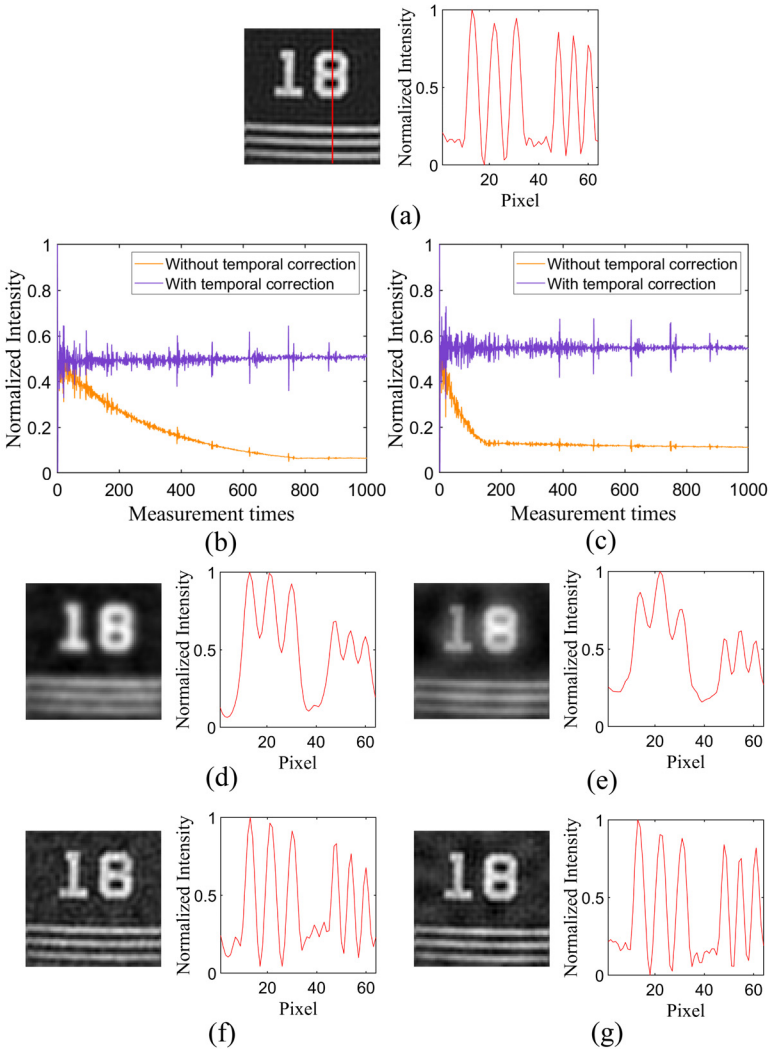

FIG. 4. Static and clean water environment: (a) a reconstructed object image (64 × 64 pixels) and a normalized intensity curve along the 42nd column (indicated by a red line) of the reconstructed object image. Dynamic and complex scattering media: (b) and (c) the normalized single-pixel light intensities without and with temporal corrections as slow and fast turbidity changes, respectively, happen over the first 1000 measurements, (d) and (f) the reconstructed object images (64 × 64 pixels) and the normalized intensity curves, respectively, without and with temporal corrections using a slow milk dripping rate in the funnel, and (e) and (g) the reconstructed object images (64 × 64 pixels) and the normalized intensity curves, respectively, without and with temporal corrections using a fast milk dripping rate in the funnel.

28 May 2025 01:55:27

Published under an exclusive license by AIP Publishing

can be corrected, and the corrected realizations $\tilde{B}_i$ can be obtained by

$$\tilde{B}_i = \frac{B_i}{B_{ti}} = \frac{k_i \int\int I_i(x,y)G(x,y)dxdy}{k_{ti} \int\int T(x,y)G(x,y)dxdy} \approx \frac{1}{\rho}\hat{B}_i. \quad (5)$$

Then, spectrum $F(u,v)$ can be calculated by using four-step phase-shifting[8,9] via phase modulation in the illumination patterns, and a reconstructed object image $\bar{G}(x,y)$ is obtained by using inverse fast Fourier transform (IFFT). The derivations are shown in Eqs. (S2) and (S3) in the supplementary material,

$$F(u,v) = (\tilde{B}_{i\to 0} - \tilde{B}_{i\to \pi}) + j(\tilde{B}_{i\to 0.5\pi} - \tilde{B}_{i\to 1.5\pi}), \quad (6)$$

$$\bar{G}(x,y) = \mathrm{Re}\{\mathrm{IFFT}[F(u,v)]\}, \quad (7)$$

where $j = \sqrt{-1}$ and Re denotes a real part.

A series of optical experiments are conducted to illustrate the feasibility of the proposed method. With the Floyd–Steinberg error diffusion dithering algorithm that sacrifices at least half of the whole spatial resolution to approximate binary patterns from gray-scale ones, the illumination patterns are resized from 64×64 pixels to 128×128 pixels, followed by a $2\times$ digital zoom to be of 256×256 pixels.

The resolving power of the developed single-pixel microscopic imaging system is also evaluated by using the Rayleigh criterion. The coefficient[16,28] R is calculated by

$$R = \max\left(\frac{P_2}{\min(P_1,P_3)}, \frac{P_4}{\min(P_3,P_5)}\right), \quad (8)$$

where $P_1 \sim P_5$ denote the extrema on an intensity curve as indicated in Fig. 3. When coefficient[16,28] R is not larger than 0.81 [see Eq. (S4) in the supplementary material], the bars are considered to be distinguishable. The smaller coefficient R means that it can be easier to distinguish a reconstructed object image.

The sparsity of object information in the Fourier domain can lead to rationality of the reconstruction using only partial spectra in the developed single-pixel microscopic imaging system. A reconstructed object image, the selected spectra, and a normalized intensity curve along the 32nd column of the reconstructed object image are shown in Fig. 3(a), when only static and clean water tank is placed in the optical path. The reconstructed object image is of high quality, and the coefficient R is 0.187. Figure 3(b) shows experimental results, when a complex scattering environment in Fig. 1 is applied and 50-ml diluted milk suspension is used during the measurements. It is illustrated that the reconstructed object image becomes blurred when optical waves propagate through dynamic and complex scattering media, significantly suppressing high-frequency information. As dynamic scattering media are increasingly turbid, contemporaneous spatial-frequency information is suppressed. In Fig. 3(b), the coefficient R is 0.718, indicating that the bars are nearly indistinguishable. When the proposed temporal correction method is applied in the developed single-pixel microscopic imaging through dynamic and complex scattering media, Fig. 3(c) shows a substantial enhancement in spectral restoration and image quality. The coefficient R is 0.191, which is close to that obtained in single-pixel microscopic imaging through static and clean water. Group 5 Element 5 of USAF 1951 resolution test chart with a linewidth of 9.84 μm is resolved. The detailed analyses using different percentages of spectra are given in Fig. S1 in the supplementary material.

The varying speed of turbidity in water tank is further investigated by adjusting the milk dripping rate in the funnel, and 50-ml diluted milk suspension is used. Figure 4(a) shows the experimental reconstruction result with an intensity curve to serve as a comparison benchmark, when only static and clean water is used in the optical path. Figures 4(b) and 4(c) show the first 1000 normalized light intensities (with and without temporal corrections), when slow and fast milk dripping rates are adopted, respectively. The blurring occurs even when turbidity changes slowly in a random manner, as shown in Fig. 4(d). When the turbidity varies rapidly, the reconstructed object images become heavily blurred and high frequency is suppressed as shown in Fig. 4(e). Despite a change of the turbidity in dynamic scattering environments, the proposed method can be applied to reconstruct high-quality object images, as shown in Figs. 4(f) and 4(g). It is experimentally verified that the proposed method is feasible and effective.

To further verify the feasibility of the proposed method, biological specimens are also tested as shown in Figs. 5(a)–5(c). When static and clean water is placed in the optical path, high imaging quality with clear edges is achieved. In dynamic and complex scattering media, the reconstructed object images become blurred. When the proposed method is applied, the reconstructed object images are of high quality. The detailed analyses using different percentages of spectra are given in Fig. S2 in the supplementary material. In addition, it can be expected[29] that

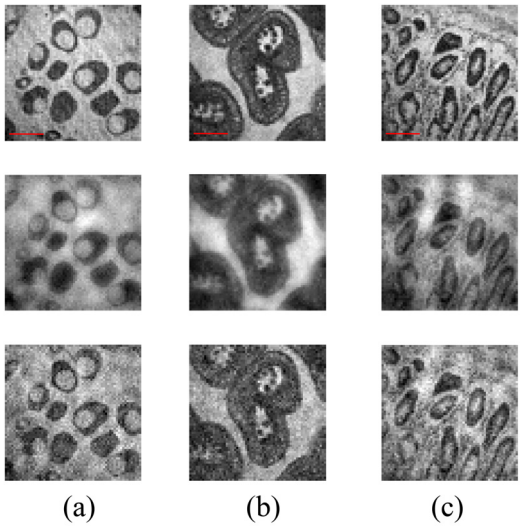

FIG. 5. (a) Testis of Fish T.S., (b) Apical bud L.S., and (c) Frog Intestine Sec. These experimental results (64×64 pixels) are obtained through static and clean water (top row), complex scattering media without temporal carriers (middle row), and complex scattering media with temporal carriers (bottom row), respectively. 100% spectra are employed. Scale bar: 100 μm.

28 May 2025 01:55:27

Published under an exclusive license by AIP Publishing

the proposed method can be extended to three-dimensional (3D) domain in complex and dynamic scattering environments.

In conclusion, we have reported an approach to realizing high-resolution single-pixel optical microscopic imaging through complex scattering media. The experimental results with artificial targets and biological specimens demonstrate that frequency information has been significantly suppressed, when optical waves propagate through thick, dynamic, and complex scattering media. This challenge is effectively overcome by employing the proposed temporal corrections with a fixed carrier to remove the effect of dynamic scaling factors, showing potential for the development of high-resolution optical microscopic imaging through various dynamic and complex scattering media.

See the supplementary material for the methods and more experimental results.

This work was supported by the Hong Kong Research Grants Council (Nos. 15224921 and 15223522) and the Hong Kong Polytechnic University (Nos. 1-CDJA and 1-WZ4M).

AUTHOR DECLARATIONS

Conflict of Interest

The authors have no conflicts to disclose.

Author Contributions

Tianshun Zhang: Data curation (lead); Formal analysis (lead); Investigation (lead); Methodology (lead); Writing – original draft (lead). **Yin Xiao:** Formal analysis (lead); Investigation (lead). **Wen Chen:** Conceptualization (lead); Formal analysis (lead); Methodology (lead); Project administration (lead); Supervision (lead); Writing – review & editing (lead).

DATA AVAILABILITY

The data that support the findings of this study are available from the corresponding author upon reasonable request.

REFERENCES

[1]S. L. Jacques, "Optical properties of biological tissues: A review," Phys. Med. Biol. **58**, R37 (2013).
[2]V. Kalchenko, D. Preise, M. Bayewitch, I. Fine, K. Burd, and A. Harmelin, "In vivo dynamic light scattering microscopy of tumour blood vessels," J. Microsc. **228**, 118–122 (2007).
[3]X. Gao, C. Zhang, and X. Li, "Computational underwater ghost imaging based on scattering-and-absorption degradation," Opt. Lett. **49**, 4461–4464 (2024).
[4]Y. Peng and W. Chen, "Deep learning-enhanced ghost imaging through dynamic and complex scattering media with supervised corrections of dynamic scaling factors," Appl. Phys. Lett. **124**, 181104 (2024).
[5]Q. Song, Q. H. Liu, and W. Chen, "High-resolution ghost imaging through dynamic and complex scattering media with adaptive moving average correction," Appl. Phys. Lett. **124**, 211104 (2024).
[6]Y. Xiao, L. Zhou, and W. Chen, "High-resolution ghost imaging through complex scattering media via a temporal correction," Opt. Lett. **47**, 3692–3695 (2022).
[7]M. P. Edgar, G. M. Gibson, and M. J. Padgett, "Principles and prospects for single-pixel imaging," Nat. Photonics **13**, 13–20 (2019).
[8]Z. Zhang, X. Ma, and J. Zhong, "Single-pixel imaging by means of Fourier spectrum acquisition," Nat. Commun. **6**, 6225 (2015).
[9]Z. Zhang, X. Wang, G. Zheng, and J. Zhong, "Fast Fourier single-pixel imaging via binary illumination," Sci. Rep. **7**, 12029 (2017).
[10]R. Sun, J. Long, Y. Ding, J. Kuang, and J. Xi, "Hadamard single-pixel imaging based on positive patterns," Photonics **10**, 395 (2023).
[11]G. Huang, Y. Shuai, Y. Ji, X. Zhou, Q. Li, W. Liu, B. Gao, S. Liu, Z. Liu, and Y. Li, "Compressed Hermite–Gaussian differential single-pixel imaging," Appl. Phys. Lett. **124**, 111108 (2024).
[12]Y. Hao and W. Chen, "A dual-modality optical system for single-pixel imaging and transmission through scattering media," Opt. Lett. **49**, 371–374 (2024).
[13]Y. Wu, P. Ye, I. O. Mirza, G. R. Arce, and D. W. Prather, "Experimental demonstration of an optical-sectioning compressive sensing microscope (CSM)," Opt. Express **18**, 24565–24578 (2010).
[14]Y. N. Zhao, H. Y. Hou, J. C. Han, S. Gao, S. W. Cui, D. Z. Cao, B. L. Liang, H. C. Liu, and S. H. Zhang, "Single-pixel phase microscopy without 4f system," Opt. Lasers Eng. **163**, 107474 (2023).
[15]Y. Wang, D. Wu, M. Yang, S. Bai, S. Huang, M. Wang, R. Liu, Z. Li, D. Li, and Y. Shen, "Microscopic single-pixel polarimetry for biological tissue," Appl. Phys. Lett. **122**, 203701 (2023).
[16]X. H. Zhu, Y. F. Bai, W. Tan, L. Y. Zhou, X. W. Huang, T. J. Jiang, T. Jiang, S. Q. Nan, and X. Q. Fu, "High-resolution microscopic ghost imaging for bioimaging," Phys. Rev. Appl. **20**, 014028 (2023).
[17]Y. Wang, F. Wang, R. Liu, P. Zhang, H. Gao, and F. Li, "Sub-Rayleigh resolution single-pixel imaging using Gaussian-and doughnut-spot illumination," Opt. Express **27**, 5973–5981 (2019).
[18]Y. Liu, J. Suo, Y. Zhang, and Q. Dai, "Single-pixel phase and fluorescence microscope," Opt. Express **26**, 32451–32462 (2018).
[19]C. Ahn and J. H. Park, "Confocal single-pixel imaging," Photonics **10**, 687 (2023).
[20]A. M. Caravaca Aguirre, F. Poisson, D. Bouchet, N. Stasio, P. Moreau, I. Wang, E. Zhang, P. Beard, C. Prada, and C. Moser, "Single-pixel photoacoustic microscopy with speckle illumination," Intell. Comput. **2**, 0011 (2023).
[21]N. Radwell, K. J. Mitchell, G. M. Gibson, M. P. Edgar, R. Bowman, and M. J. Padgett, "Single-pixel infrared and visible microscope," Optica **1**, 285–289 (2014).
[22]M. Yao, Z. Cai, X. Qiu, S. Li, J. Peng, and J. Zhong, "Full-color light-field microscopy via single-pixel imaging," Opt. Express **28**, 6521–6536 (2020).
[23]A. Ebner, P. Gattinger, I. Zorin, L. Krainer, C. Rankl, and M. Brandstetter, "Diffraction-limited hyperspectral mid-infrared single-pixel microscopy," Sci. Rep. **13**, 281 (2023).
[24]A. Rodríguez, P. Clemente, E. Tajahuerce, and J. Lancis, "Dual-mode optical microscope based on single-pixel imaging," Opt. Lasers Eng. **82**, 87–94 (2016).
[25]J. Peng, M. Yao, Z. Huang, and J. Zhong, "Fourier microscopy based on single-pixel imaging for multi-mode dynamic observations of samples," APL Photonics **6**, 046102 (2021).
[26]P. Hong and Y. Liang, "Three-dimensional microscopic single-pixel imaging with chaotic light," Phys. Rev. A **105**, 023506 (2022).
[27]H. Deng, G. Wang, Q. Li, Q. Sun, M. Ma, and X. Zhong, "Transmissive single-pixel microscopic imaging through scattering media," Sensors **21**, 2721 (2021).
[28]L. Rayleigh, "Investigations in optics, with special reference to the spectroscope," Philos. Mag. **8**, 261 (1879).
[29]Y. Liu, P. Yu, Y. Wu, J. Zhuang, Z. Wang, Y. Li, P. Lai, J. Liang, and L. Gong, "Optical single-pixel volumetric imaging by three-dimensional light-field illumination," Proc. Natl. Acad. Sci. U. S. A. **120**, e2304755120 (2023).

28 May 2025 01:55:27

Published under an exclusive license by AIP Publishing